# Temperature Modelling of the Synthesis of Oxide Nanoparticles by Ultrasonic Spray Pyrolysis

Jelena Bogovic, Srećko Stopić, Jacqueline Gruber, Herbert Pfeifer, Bernd Friedrich

Nanosized particles of spherical titanium dioxide were prepared from an aerosol based on an organometallic solution during ultrasonic spray pyrolysis. The influence of process parameters on particle morphology was considered. During the aerosol generation, the droplet size distribution was measured with a laser diffraction system (Malvern Spraytec) without dilution of the aerosol and for the same atomization and carrier gas parameters as those during the synthesizing process. By carrying out a series of experiments the influences of different process parameters (gas flow rate, decomposition temperature, retention time, etc.) on particle size, distribution and morphology were tested. Obtained nanoparticles were characterized using various methods (SEM, EDS, and SMPS) with respect to structure and composition. The goal was to determine the most sensitive process steps and to propose solutions for improvement of the critical points. Measurements and numerical simulation of temperature profile in different heating zones was done, in order to better understand the process steps in each heating zone. A reaction mechanism of synthesis is proposed, as well as optimal experimental conditions for preparation of nanopowder with a specific particle size distribution and morphology.

Keywords:

Nanosized titanium dioxide – Ultrasonic spray pyrolysis – Particle morphology – Numerical simulation – Nanopowder

**Temperaturmodellierung der Synthese oxidischer Nanopartikel durch Ultraschallsprühpyrolyse**

Im Rahmen dieser Arbeit wurden Nanopartikel von sphärischem Titandioxid aus einem Aerosol basierend auf einer metallorganischen Lösung durch Ultraschallsprühpyrolyse hergestellt. Es wurde die Einflussnahme gewisser Prozessparameter auf die Partikelmorphologie vermutet. Während der Aerosolerzeugung wurde die Tröpfchengrößenverteilung durch ein Laserbeugungssystem (Malvern Spraytec) ohne Verdünnung des Aerosols und für dieselben Atomisierungs- und Trägergasparameter wie jene während des synthetisierenden Prozesses gemessen. Durch eine Versuchsserie wurden die Einflüsse verschiedener Prozessparameter (Volumenstrom, Zerlegungstemperatur, Haltedauer usw.) auf die Teilchengröße, Verteilung und Morphologie getestet. Struktur und Zusammensetzung des durch die Ultraschallsprühpyrolyse hergestellten Nanopulvers wurden mit Hilfe von verschiedenen Methoden (SEM, EDS und SMPS) charakterisiert. Das Ziel sollte die Bestimmung der empfindlichsten Prozessschritte und die Lösungsfindung für deren Verbesserung sein. Um die verschiedenen Prozessschritte, die in den jeweiligen Heizzonen ablaufen, verstehen zu können, wurden Messungen und numerische Simulationen durchgeführt. Vorgeschlagen werden sowohl ein Reaktionsmechanismus zur Synthese als auch die optimalen Versuchsbedingungen zur Herstellung des Nanopulvers einer bestimmten Teilchengrößenverteilung und Morphologie.

Schlüsselwörter:

Nanogroßes Titandioxid – Ultraschallsprühpyrolyse – Partikelmorphologie – Numerische Simulation – Nanopulver

**Modélisation de la température pour la synthèse de nanoparticules d'oxyde par pyrolyse par pulvérisation à ultrasons**

**Modelo de temperatura para la síntesis de nanopartículas de óxido por Pirólisis Ultrasónica**

This is a peer-reviewed article

## 1 Introduction

Titanium dioxide ($TiO_2$) is a material with various applications. Because of its high refractive index, inertness and colour, titanium dioxide is widely used as a pigment. This is one of its most common applications where $TiO_2$ is used in particle form. Some newer $TiO_2$ applications are a result of its photo-catalytic and semiconducting properties, for example photo degradation of organic pollutants, water purification, waste water treatment, air purification or utilisation in solar cells and self-cleaning paints. Titanium dioxide can be produced using various synthetic methods, such as the sol-gel method, vapour decomposition and different hydrothermal techniques [1-3]. In the case of hydrothermal methods, the process can be divided in the following main steps:

- preparation of precursor (titanium salt solution),
- thermal decomposition, where several heat sources can be applied (e.g. flame, wall heated reactor, plasma),
- particle generation, and finally
- nanopowder collection.

Ultrasonic spray pyrolysis represents nanopowder production from an aerosol based on precursor atomisation (droplet size 1 to 100 µm), aerosol transport through a temperature and atmosphere regulated reactor. Particle morphology in these processes is a result of droplet size, precursor concentration and physical characteristics, operating temperature and evaporation rate [4]. In order to obtain a certain particle size and morphology, heating grade, evaporation rate, retention time and other process specific parameters have to be known and controlled. Inside the furnace it is assumed that the following steps are taking place: evaporation of solvent, diffusion of solutes, precipitation, decomposition and densification [4]. These process steps are simplified and their understanding is imperative for controlling the particle formation process. Most previous investigation took process temperature, droplet size and evaporation rate as the main parameters that influence particle morphology [5-7]. Based on these assumptions Jayanthi et al. defined relative time constants for different process steps in their model and have shown that droplet shrinkage and solute diffusion are the slowest steps [6].

In the present work the influence of the main parameters (temperature, flow rate) on $TiO_2$ nanopowder was tested by a series of experiments [8]. The main aim was to produce spherical nanoparticles in a size range of 100 to 300 nm, with high homogeneity of particle size distribution. Particle size was regulated by droplet size and precursor concentration. The morphology was determined in dependence of the temperature and carrier gas flow rate mainly through first two process steps – evaporation and precipitation. Since temperature is an important factor in particle formation, the temperature profile inside the furnace was measured and in addition a numerical simulation model of the reactor was created using the software ANSYS FLUENT 13.0. The second parameter with an influence on particle morphology – the carrier gas flow rate – also has an influence on the productivity of the process. By increasing the carrier gas flow rate more precursor solution can be transported in the form of aerosol and this way more nanopowder can be produced. For this reason it was interesting to investigate maximal flow rates for which the kinetics of the separate process steps is still suitable for the formation of particles with a spherical morphology. It was expected that the carrier gas flow rate is limited by its influence on the evaporation rate. This relationship was also investigated and optimal conditions based on experimental results were proposed.

## 2 Experimental

The precursor solution that was used for the synthesis of $TiO_2$ nanopowder by USP was tetra-n-butylorthotitanate $C_{16}H_{36}O_4Ti$ (Merck, Darmstadt, Germany). Equipment used for the experiments is described in previous work of Bogovic et al. [8-9] and is shown in Figure 1.

The whole USP process can be separated into the three main process steps (aerosol generation, thermal decomposition, nanopowder collection). The process begins with aerosol generation through atomisation of a precursor solution in an ultrasonic atomizer (Gapusol 9001, RBI/France) with three transducers operating at a resonant frequency of 2.5 MHz. This generator is specially developed with a goal to increase aerosol production and in this way also increase the nanopowder production rate. Droplet size distributions were measured without dilution of the aerosol and with the same atomization and carrier gas parameters as those of the synthesizing process (Institute of Process Engineering in Life Sciences, Section I: Food Process Engineering, Karlsruhe Institute of Technology (KIT)). A laser diffraction system (Malvern Spraytec) equipped with a 300 mm focusing lens was utilized for these investigations. Size measurement by laser diffraction is based on the size

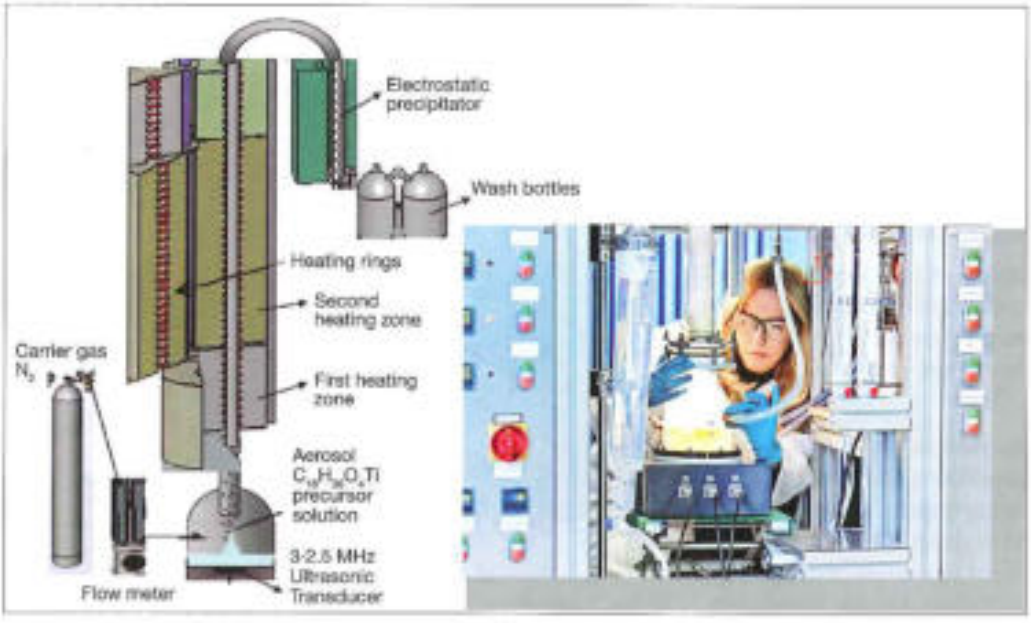


Fig. 1:
Experimental set-up and details of 3-2.5 MHz ultrasonic transducer

dependent scattering angle of light at a droplet or particle and therefore the scattering signal from the aerosol is detected in order to determine the droplet size distribution. Generated aerosol is carried into the reaction zone with a nitrogen flow rate 3.5 to 10 l/min. The reaction zone (quartz tube l = 1.8 m, d = 42 mm) is situated in a furnace with three separately regulated heating zones with a temperature range 0 to 1100 °C. The so-called "pre-heating" zone and "cooling" zone are situated at the entrance and exit of the furnace, each with a length of 0.4 m, and in the middle is the "reaction" zone with a length of 1 m. The whole system was under inert atmosphere and is slightly below atmospheric pressure (980 mbar). This measurement was done with a goal to determine droplet size distribution and also determine if more transducers in one generator have an influence on droplet formation. For nanopowder collection an electrostatic precipitator was used. Characterisation of the obtained titanium dioxide nanopowder was done using a scanning electron microscope. SEM images were used for the observation of particle morphology, structure, size and size distribution. A qualitative analyses of the powders obtained was done by energy disperse spectroscopy (EDS) analysis with a Si(Bi) X ray detector, connected with SEM and a multi-channel analyzer. Particle size and particle size distribution was determined with on-line measurements with SMPS Scanning Mobility Particle Sizer system with DMA Differential Mobility Analyser (Grimm, Germany) after the second heating zone and once more after the powder collection by SEM image analyses with ImageJ softer, while experimental data were processed by the computer program Origine8 [8].

Experimental conditions for the preparation of $TiO_2$ nanopowder are given in Table 1. The aim of the experiments was to determine the influence of evaporation rate, temperature and carrier gas flow rate on morphology and particle size of the produced nanopowder. All experiments were conducted with 6 g/l $C_{16}H_{36}O_4Ti$ precursor solution.

Table 1: Experimental conditions for the three heating zones of the pyrolysis reactor

| Experiment | Temp. [°C] | $N_2$ [l/min] |
|---|---|---|
| 1 | 800-800-300 | 4 |
| 2 | 800-800-300 | 7 |
| 3 | 800-800-300 | 10 |
| 4 | 300-800-300 | 4 |
| 5 | 300-800-300 | 7 |
| 6 | 300-800-300 | 10 |

The influence of the concentration of the precursor solution on oxidic nanoparticles was studied in previous works [9-10]. Based on these results, the lowest concentration possible was selected in order to obtain nanopowder in the specific particle size range.

Experimental data were chosen in order to test the influence of different evaporation conditions on particle formation. Carrier gas flow rate and temperature were regulated in order to simulate evaporation of droplets in low and high temperature zone, and for different velocities of droplets in these zones. Since the goal of titanium dioxide nanoparticle production was to produce spherical nanoparticle with maximal homogeneity, in the size range 100 to 300 nm, the particle size distribution was also determined.

## 3 Numerical Simulation

In addition to the experimental investigations described above, measurements of the temperature distribution of the carrier gas within the quartz glass reactor tube were carried out. In order to do so, the insulation section above heating zone 3 was opened and the top elbow section of the quartz glass reactor tube was removed. This made it possible to lower a thermocouple into the carrier gas flow and measure the approximate temperature distribution along the entire length of the 1.8 m long reactor. These measurements were used to validate the results of a numerical simulation model created using the software ANSYS FLUENT 13.0. The geometry and individual components of the numerical model are shown in Figure 2.

The measurements and numerical simulations were carried out in order to obtain more detailed information on the thermal conditions to which the droplets and particles are subjected in the reactor. This information makes it possible to better interpret the experimental results by considering the influence of the temperature distribution of the individual components within the reactor on the particle formation process.

As can be seen in Figure 2, the model starts at the inflow of the carrier gas $N_2$ into the first heating zone (HZ1) and ends shortly after the outflow of the carrier gas out of heating zone 3 (HZ3). Not only the separate heating elements in each heating zone, but also the air gap between the quartz glass tube with an external diameter of 48 mm and the insulation material which has an internal diameter of 62 mm as well as the approximately 3 mm high air gap between heating zone 1 and 2 and heating zone 2 and 3 are

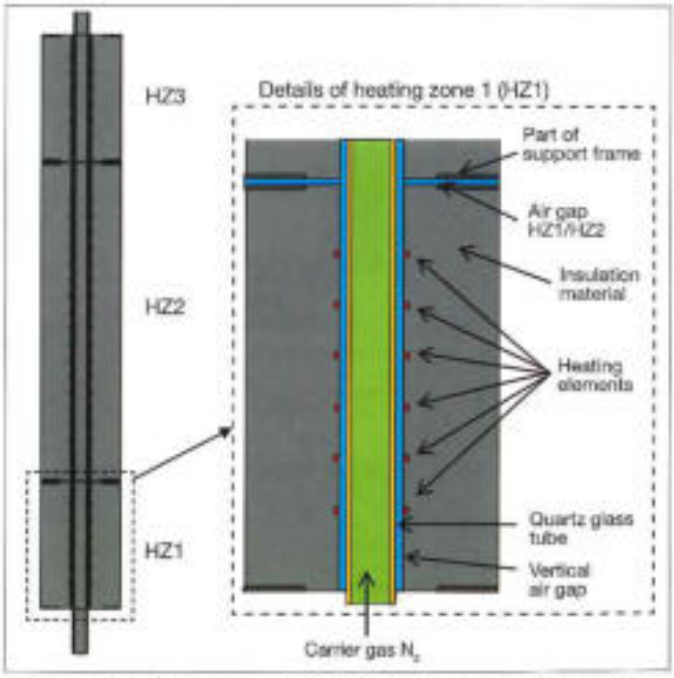


Fig. 2: Geometry and components of the numerical simulation model

included in the model. A laminar flow for both the carrier gas and air inflow with an initial temperature of 25 °C is assumed. The thermal radiation within the air gaps, through the quartz glass tube and carrier gas is simulated using the discrete ordinates (DO) thermal radiation model, whereby the thermal absorption coefficient of the quartz glass tube is defined as a function of temperature. Whereas the carrier gas and air are transparent as far as thermal radiation is concerned, the quartz glass absorbs thermal radiation in dependence of the wavelength. Wien's displacement law was used to obtain a relationship between the wavelength of the thermal radiation and the temperature of the tube, in order to estimate the amount of thermal radiation absorbed by the quartz glass. The cooling of the external surfaces of the insulation material due to convection and thermal radiation to the surroundings is taken into account. The carrier gas $N_2$ flows into the reactor with a volume flow rate of 7 l/min and a temperature of 25 °C. The boundary conditions of the model correspond to the experimental setup when the insulation section above heating zone 3 is open and the top elbow section of the quartz glass reactor tube is removed. A numerical simulation was carried out for the heating zone set point temperatures of 300/800/300 °C (Case 1) and 800/800/300 °C (Case 2). For Case 1 the heating power of the heating zones 1, 2 and 3 is set to 102 W (17 % of max. power), 1320 W (44 % of max. power) and 0 Watt respectively. For Case 2 the heating power of the heating zones 1, 2 and 3 is set to 300 W (50 % of max. power), 1065 W (36 % of max. power) and 0 W respectively. The inflow of air into the gaps for each case was found by iteration, whereby the results of the simulation were compared to the measured carrier gas temperatures and the set point temperatures of each heating zone.

## 4 Results and discussion

Ultrasonic spray pyrolysis is based on the assumption that from each droplet one particle is produced and that all droplets are going through the same process steps with the same conditions [10-11]. For this reason, the first step in particle size distribution determination is to determine droplet size distribution. Droplet size distribution is presented in Figure 3, for 6 g/l $C_{16}H_{36}O_4Ti$ precursor solution and 3-2.5MHz transducer [8].

When considering the droplet size distribution it is obvious that there is no single value of droplet size, instead a droplet size distribution must be used, where droplets are within the range 1 to 15 µm, with the highest probability of droplet diameter within the range of 4 to 6 µm. By knowing the droplet size distribution, it is expected to get a similar distribution of particle size, but in the range of 100 to 400 nm. In theory, there is a model to predict average droplet size, by knowing the influence of physical properties of the atomized solution and frequency of the ultrasound and it was studied by Lang et al. [12]. Their model results in the following formula:

$$D = 0{,}34 \cdot \left( \frac{8 \cdot \pi \cdot \gamma}{\rho \cdot f^2} \right)^{\frac{1}{3}} \quad (1)$$

(D: mean droplet diameter; γ: surface tension of the solution; ρ: density of the solution; f: ultrasound frequency )

After measuring surface tension and density of the precursor solution, the average droplet size corresponding to the frequency used was calculated to be 2.8 µm. When this value is compared with the experimental result (4 to 6 µm), it can be concluded that the theoretical average droplet size is not adequate and for this reason the theoretical model is not going to be used in further investigations. A reason for this might be coagulation that occurs between droplets in the tube that connects the generator with the furnace. In the theoretical formula the influence of coagulation is not taken into account. It is possible that the coagulation rate is also influenced by the generator construction, application of multiple transducers and experimental parameters. For this reason in this paper droplet size distribution was measured for the specific generator used during the experiments and for the relevant experimental parameters. All conclusions in this paper are therefore based only on experimental results and based on these a model is going to be proposed. After conducted experiments, first information concerning the produced nanopowder can be obtained from SEM (Scanning Electron Microscopy) images. SEM images were used to observe the surface morphology of particles formed for different experimental parameter sets and to obtain first information about particle size distribution range. SEM images of the powders produced during the experiments are given in Figure 4 and Figure 5. [8]

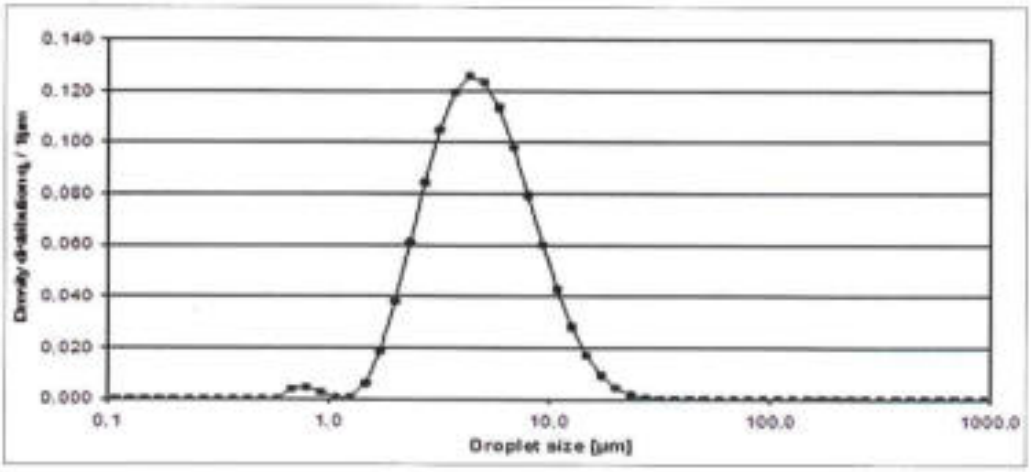


Fig. 3:
Droplet size distribution

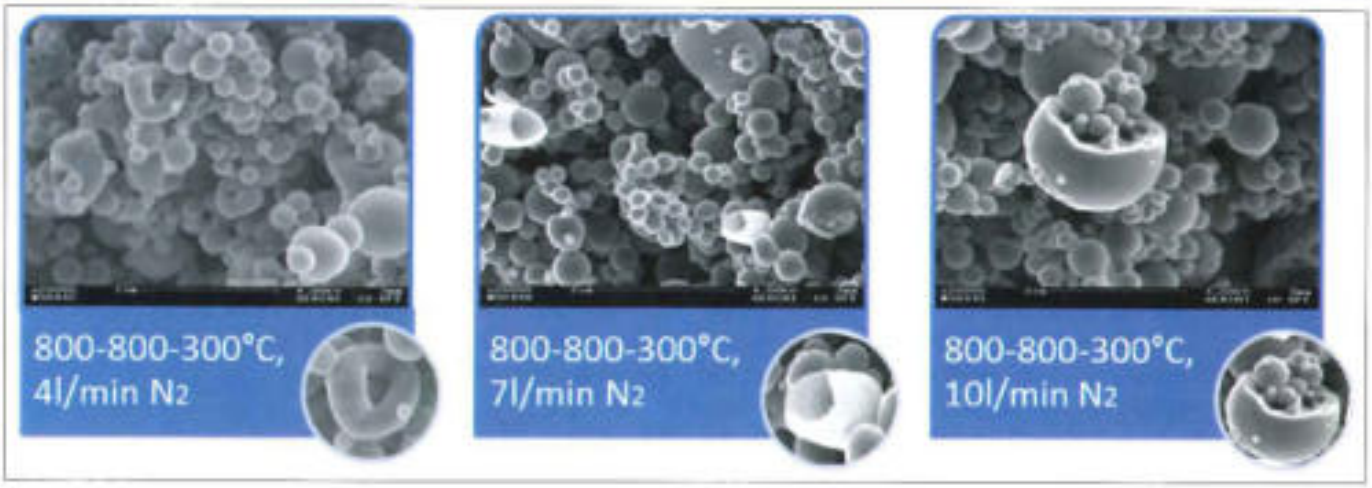


Fig. 4: SEM analysis from titanium dioxide nanopowder obtained in experiments 1 to 3 (left and right are SEM images of same experiment)

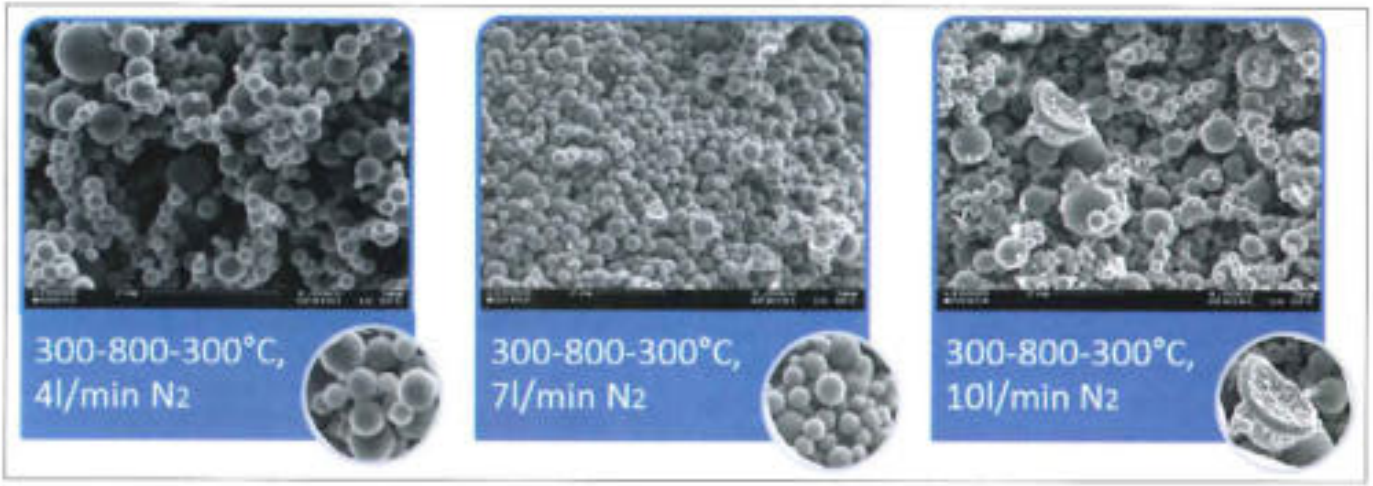


Fig. 5: SEM analysis from titanium dioxide nanopowder obtained in experiments 4 to 6 (left and right are SEM images of same experiment)

By considering the presented results, it can be concluded that the nanopowder produced in the first three experiments (Figure 4, temperature in first heating zone is regulated to be 800 °C) consists mainly of spherical particles and a certain number of particles in irregular form. In the first experiment, image left, we can see "settle" like particles with a hole in the middle. In the second and third experiment, with higher flow rate of carrier gas, we can see a broken, "exploded" nanoparticle with "caves" inside its structure. As shown in Figure 4, in which results of experiments with a set point temperature in the first heating zone of 300 °C are presented, we can see that most of the particles in the obtained powder have a spherical shape. Few examples of destroyed particles can be seen in the last experiment, with a higher flow rate. It is assumed that due to the high flow rate, particles enter the reaction zone and high temperature before evaporation and precipitation steps are finished and this might be the reason for particle destruction.

It is obvious when examining the particles, that the thermal conditions in the reactor play an important part in the particle formation. Therefore, as described before in section 3 of this paper, the temperature profile of the inert gas $N_2$ along the length of the reactor for both temperature regulations (set point temperature settings) was measured and in addition numerical simulation calculations to determine the thermal conditions in the reactor were carried out. In Figure 6 the measured temperature profiles are compared to those calculated using the numerical simulation model.

From Figure 6 it can firstly be concluded that the simulated temperature profiles of the inert gas at the inner surface of the reactor wall and in the centre of the reactor correspond sufficiently well with the measured temperature profiles. It can also be concluded that the measured temperature profile in the reactor in heating zone 2 (HZ2) for both regimes looks similar. This can be confirmed by considering the simulated temperature distributions within the reactor shown in Figure 7. The difference is mainly evident in the first heating zone (HZ1).

In order to evaluate the experimental results, it is necessary to consider the thermal conditions to which the particles are subjected within the reactor. The simulated temperature profiles most relevant for particle formation within the reactor are shown in Figure 8 below. Not only are the droplets and particles subject to heating by convection along their path through the reactor, they are also heated due to the thermal radiation from the heating elements, which is partly absorbed by the quartz glass tube. This in turn also emits thermal radiation through the transparent carrier gas $N_2$ to the particles.

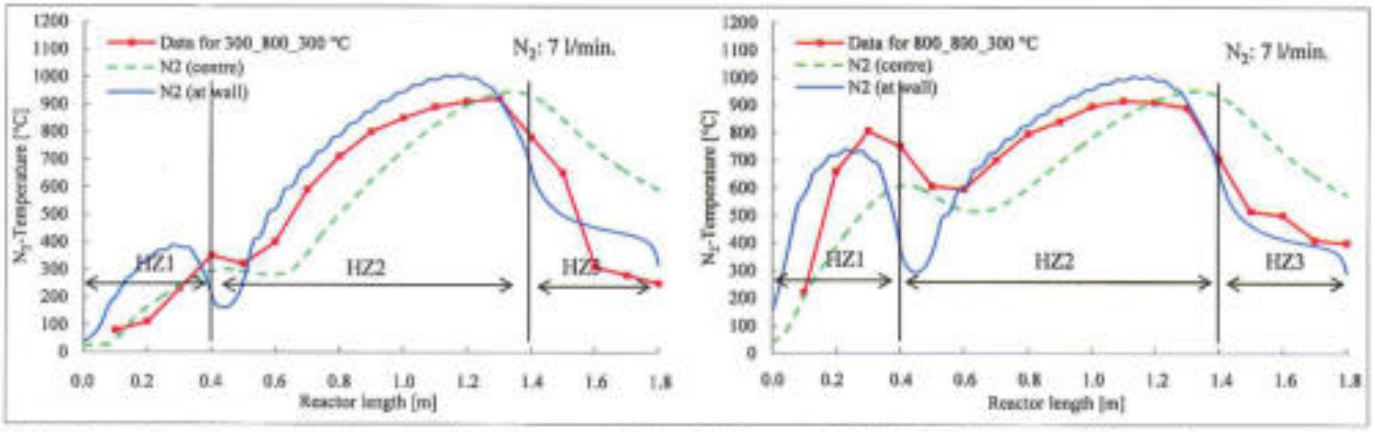


Fig. 6: Comparison of measured and simulated temperature profiles for a $N_2$ flow rate of 7 l/min for heating zone (HZ) set point temperatures of 300/800/300 °C and 800/800/300 °C

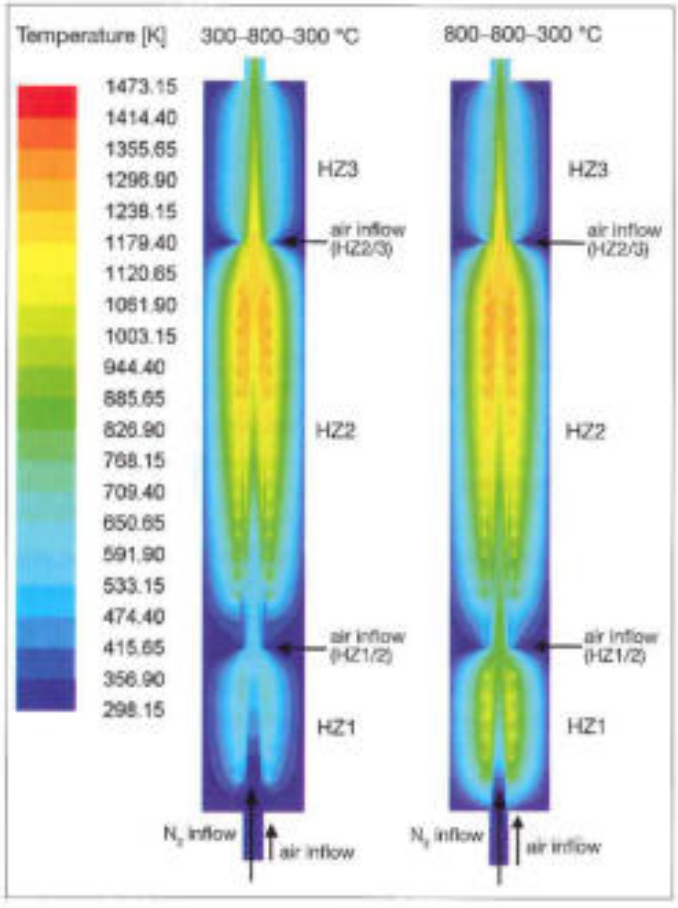


Fig. 7: A cross-section of the simulated temperature distribution within the reactor for heating zone (HZ) set point temperatures of 300/800/300 °C and 800/800/300 °C

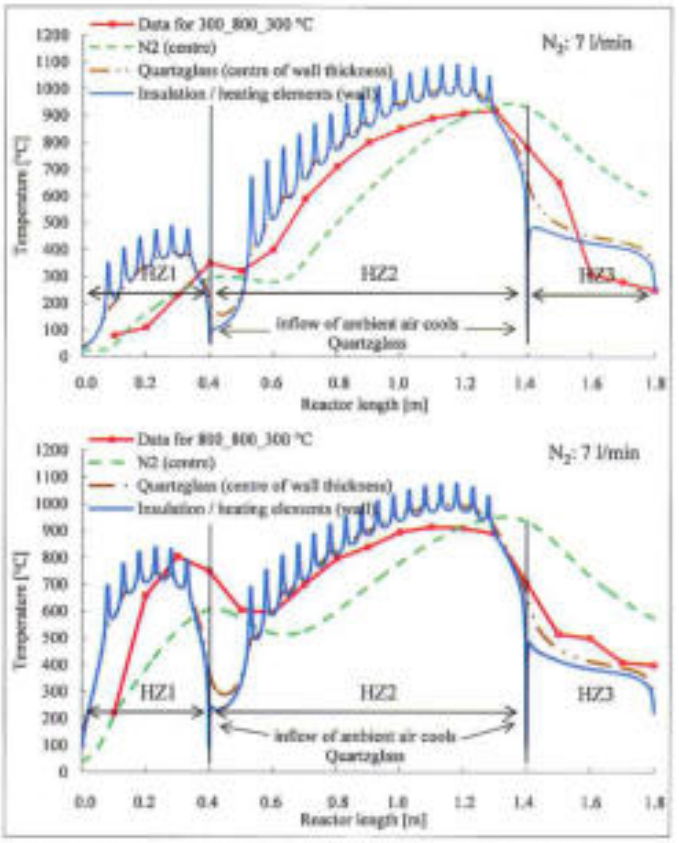


Fig. 8: Simulated temperature profiles most relevant for the particle formation for heating zone (HZ) set point temperatures of 300/800/300 °C and 800/800/300 °C

If we consider the model of particle formation, presented in Figure 9, we can see that in the first heating zone evaporation and precipitation take place. Since process parameter (temperature) in this area is significantly different, we assume that problems in the evaporation and precipitation stage are responsible for the formation of non-spherical particles.

In the following discussion the evaporation stage is analysed and its influence on the obtained powder is explained. One of the proposed explanations for the formation of hollow, "settle" and "cave" like particles is that by experimental conditions where the temperature in the first heating zone is 800 °C, the rate of evaporation is much higher than that of solute diffusion from the centre of a droplet to a surface. For this reason, the concentration of precursor in surface area rapidly increases and surface precipitation occurs. Trapped solute in the centre of droplet boils, pressure increases and the particle is destroyed or deformed.

From presented results it can be concluded that most non-spherical particle are the bigger ones. This leads to the conclusion that the size of primer droplets is also one of the parameters that influence the final particle morphology, if we assume that bigger particles are created from bigger droplets. In bigger droplets the formation of bubbles inside

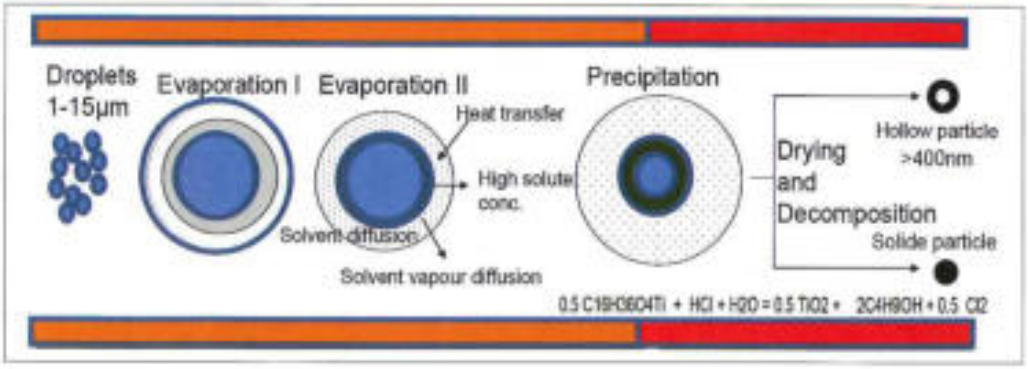


Fig. 9:
Proposed mechanisms of particle formation and decomposition reaction

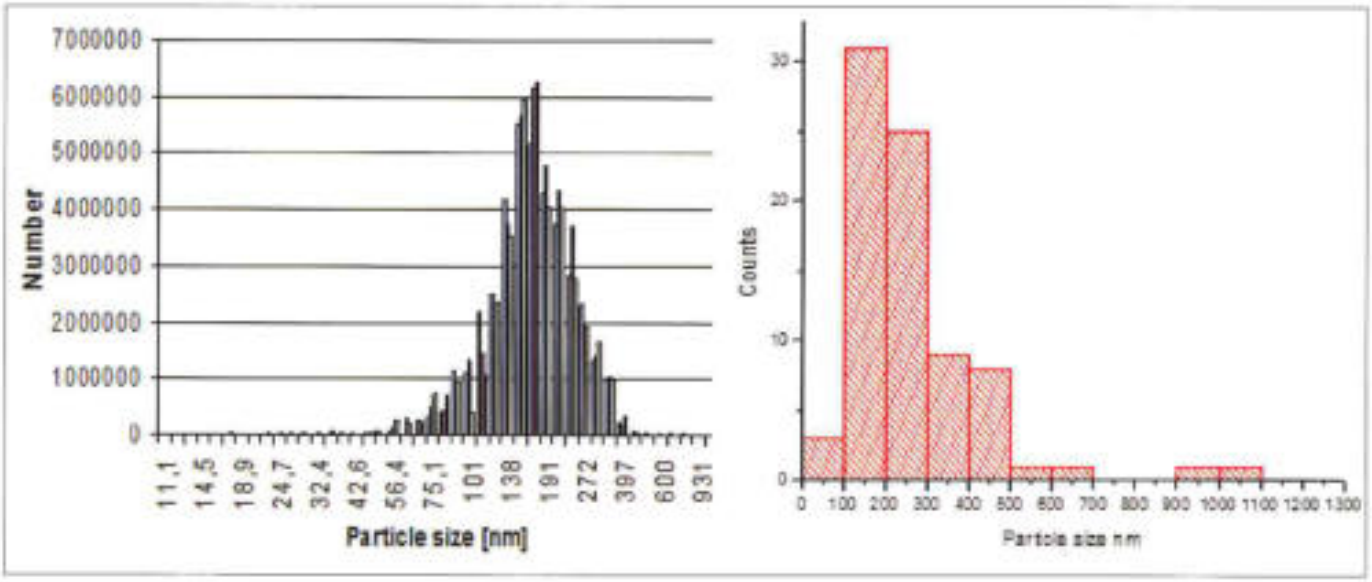


Fig. 10: SMPS on-line measurement of particle size and particle size distribution after collection of powder

a droplet during the evaporation stage is possible. Furthermore, distance dependent processes such as diffusion last longer. Unwanted effects due to a high evaporation rate were determined by experiment number 3, where a maximal carrier gas flow rate was applied. By increasing the carrier gas flow rate the droplet velocity through the reactor is increased and it reaches the area of high temperature sooner, which increases the evaporation rate at the droplet surface and leads to surface precipitation.

SMPS on-line measurement was done at the exit of the second heating zone. Thereafter the carrier gas with powder was cooled down in the third reactor zone and the powder was collected in an electrostatic precipitator. If we compare the particle size distribution at the exit of the second reaction zone and after collection, we can see that most of the particles in both distributions are within a size range of 100 to 400 nm (Figure 10). The analysis of powder after collection shows a group of particles whose diameter is bigger than 400 nm. It is possible that the number of this group is so small, that during online measurement these bigger particles were not detected. In order to obtain a narrower particle size distribution, it is necessary to produce aerosol droplets in a more narrow range. Qualitative EDS analysis of the powder has confirmed that titanium dioxide was obtained in all experiments. A characteristic result is shown in Figure 11.

Therefore it is confirmed, that even for a higher flow rate and lower retention time in the reactor there was enough time for the decomposition reaction to occur. If we look at the model of the process steps presented in Figure 7, we can see that the most sensitive process steps in these experiments were the first two process steps: evaporation and precipitation stage, since all other steps occurred with no problems occurring for all the tested experimental conditions.

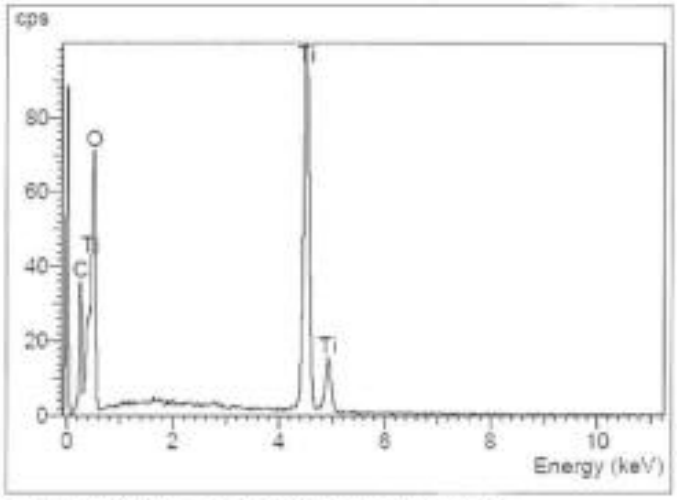


Fig. 11: EDS analyze of titanium dioxide nanopowder

## 4 Conclusions and outlook

Obtained results show that by using ultrasonic spray pyrolysis it is possible to produce spherical nanoparticles. The temperature profile and flow rate of the carrier gas are the main process parameters that influence particle morphology, where final particle sizes depend on precursor droplet size distribution and concentration, if it is assumed that every droplet undergoes the same process steps (Figure 12). Influence of coagulation of aerosol droplets, and influence of process parameters on coagulation rate was not tested in this work, but it is noted to be of interest for further investigation.

The evaporation of solute and the precipitation stages were determined to be the most sensitive stages and to have a large influence on the final particle morphology. High evaporation rate leads to surface precipitation, which means that precipitation occurs in the surface region of the droplet. This results in deformed, destroyed, non-spherical particles. The reason for this is rapid solvent evaporation and solvent vapour diffusion, compared to slow diffusion process inside the droplet.

Higher temperature and higher carrier gas flow rates lead to the production of deformed particles. These phenomena have much bigger influence on droplets with a bigger radius, due to longer diffusion path. To avoid formation of non-spherical particles it is recommended to have a reactor with a slowly increasing temperature profile.

Measurements of the temperature profile showed that separate temperature regulated zones with good temperature regulation can provide a slowly increasing temperature profile, where first two process steps are going to take place for lower temperatures and in the further process enough energy is provided for decomposition and particle formation process. In this way it is possible to optimise the process parameters in order to produce spherical nanopowder.

It is planned to continue the investigation of the particle formation process by ultrasonic spray pyrolysis in a tube reactor, by firstly creating a mathematical model which considers each step of the particle formation process and the heat and mass transfer taking place at the surface of the droplets and particles as they travel through the reactor. Thereafter it is planned to couple this mathematical model with an extended version of the numerical simulation model presented in this paper, whereby amongst other things it is planned to include the change in density of the carrier gas due to the increase in its water vapour content caused by the evaporation of the droplets. Furthermore issues such as the influence of thermal radiation and the cross-sectional velocity profile along the reactor on the particle formation process are to be addressed. The main goal of this future work is to obtain a more detailed understanding of all parts of the process, thereby making it possible to control specific process parameters in order to produce nanoparticles with different morphologies. It is expected that such a specific control of the particle morphology is going to be necessary for future applications of nanopowder.

### Acknowledgments

We would like to thank Federal State North Rhine-Westphalia and programme "NanoMikro+Werkstoffe.NER" covered by Ziel 2-Programm 2007-2013 (EFRE) for the financial support on the project "Electro-mechanic Components with new Nanoparticle Modified Noble Metal Surface Area – NanoGold". Our special thanks are addressed to our project partners Hochschule Ostwestfalen-Lippe, Lemgo, Germany and Enthone GmbH, Langenfeld, Germany.

## References

[1] Jang, H.D., Kim, S.K. & Kim, S.J. (2001): Effect of particle size and phase composition of titanium dioxide nanoparticles on the photocatalytic properties. – Journal of Nanoparticle Research, **3** (2-3), 141–147.

[2] Chang, H. et al. (2008): Synthetic routes for titania nanoparticles in the flame spray pyrolysis. – Colloids and Surfaces – A. Physicochem. Eng. Aspects, 313-314, 282-287.

[3] Guo, W. et al. (2003): Sonochemical synthesis of nanocrystalline $TiO_2$ by hydrolysis of titanium alkoxides. – Microelectronic Engineering, **66**, 95-10.

[4] Messing, G.L., Zhang, S.C. & Jayanthi, G.V. (1993): Ceramic powder synthesis by spray pyrolysis. – Aerosol Science and Technology, **19**, 478-490.

[5] Longgoro, W. et al. (2000): An experimental and modeling investigation of particle production by spray pyrolysis using a laminar flow aerosol reactor. – Journal of Materials Research, **15** (3), 733-743.

[6] Jayanthi, G.V., Zhang, S.C. & Messing, G.L. (1993): Modeling of Solid Particle Formation During Solution Aerosol Thermolysis: The Evaporation Stage. – Aerosol Science and Technology, **19**, 478-490.

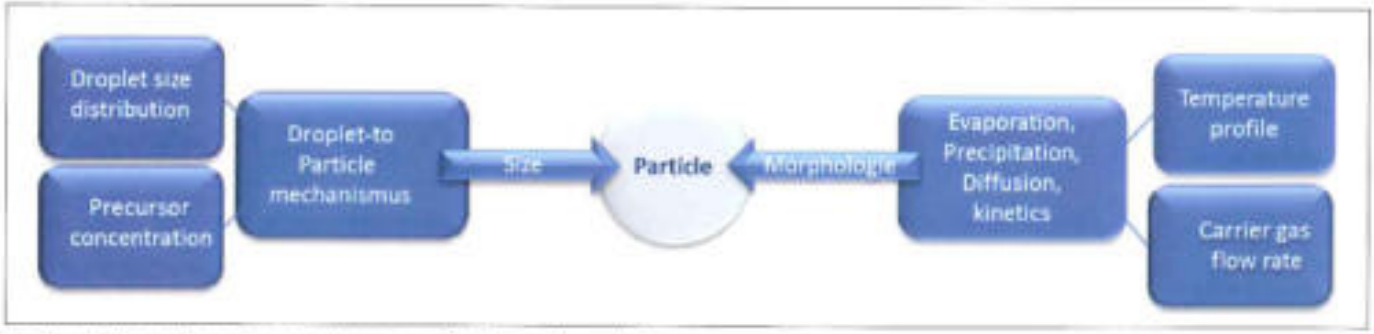


Fig. 12: Influence of process parameters on particle size and morphology

[7] Eslamin, M., Ahmed, M. & Aschoriz, N. (2006): Modelling of Nanoparticle Formation During Spray Pyrolysis. – Nanotechnology, **17**, 1674-1685.

[8] Bogovic, J., Stopic, S. & Friedrich, B. (2011): Nanosized metallic oxide produced by ultrasonic spray pyrolysis. – EMC European Metallurgical Conference, 1053-1064, Düsseldorf, Germany, ISBN 978-3-940276-38-4.

[9] Bogovic, J., Stopic, S. & Friedrich, B. (2010): Synthesis of oxidic nanoparticle by ultrasonic spray pyrolysis. – Processing and Structure of Materials, 4th International Conference, Palic, Serbia, 111-123; ISBN 978-86-87183-17-9.

[10] Jokanovic, V., Spasic, A.M. & Hsu, J.P. (2006): Stuctures and Substructures in Spray Pyrolysis. – Surfactant science series, **130**, 513-533.

[11] Tsai, S.C. et al. (2004): Ultrasonic spry pyrolysis for nanoparticles synthesis. – Journal of Materials Science, **39**, 3647-3657.

[12] Lang, R. (1962): Ultrasonic atomisation of liquids. – J. Acoust. Soc. Am., **34**, 7-10.

Dipl.-Ing. Jelena Bogovic
Dr.-Ing. Srećko Stopić
Prof. Dr.-Ing. Dr. h.c. Bernd Friedrich
All:
IME Process Metallurgy and Metal Recycling
RWTH Aachen University
Intzestraße 3
52072 Aachen
Germany
jbogovic@ime-aachen.de
sstopic@ime-aachen.de
bfriedrich@ime-aachen.de

BSc Eng., Dipl.-Ing. Jacqueline Gruber
Univ.-Prof. Dr.-Ing. Herbert Pfeifer
Both:
IOB Department for Industrial Furnaces
RWTH Aachen University
Kopernikusstraße 10
52074 Aachen
Germany
gruber@iob.rwth-aachen.de
pfeifer@iob.rwth-aachen.de